

The Comparison of InnoSAT Attitude Control Performance with the Impact of Delay Using PID-Lead, MPC-Lead, and MPC-PDLead Controllers

Fadzilah Hashim^{1*}, Siti Maryam Sharun², Mohd Yusoff Mashor³, and Nor Hasrimin Md Nor¹

¹Department of Electrical Engineering,
Politeknik Tuanku Sultanah Bahiyah,
Kulim Hi-Tech Park, 09000 Kulim, Kedah, Malaysia.

²Faculty of Innovative Design and Technology,
Universiti Sultan Zainal Abidin,
Gong Badak Campus, 21300 Kuala Nerus, Terengganu, Malaysia.

³Faculty of Electronic Engineering Technology,
Universiti Malaysia Perlis,
Pauh Putra Campus, 02600 Arau, Perlis, Malaysia.

*Corresponding Author's Email: fadzilah.hashim@ptsb.edu.my

Article History: Received 20 February 2025; Revised 13 June 2025;
Accepted 13 June 2025; Published 30 June 2025

©2025 Fadzilah Hashim et al.
Published by Jabatan Pendidikan Politeknik dan Kolej Komuniti. This is an open access article under the
CC BY-NC-ND 4.0 license (<https://creativecommons.org/licenses/by-nc-nd/4.0/>).

Abstract

The development of space technology is increasingly regarded as a strategic indicator of national progress, and Malaysia is among the emerging nations actively investing in satellite research and innovation. One of the critical challenges in satellite operations is maintaining stable attitude control in the presence of orbital disturbances. This study focuses on enhancing the stability of the Malaysian Innovative Satellite (InnoSAT), a nanosatellite platform, by improving its attitude control mechanisms. InnoSAT's control performance can be affected by various real-world factors, including time delays, sensor noise, and fluctuating system gains. To replicate realistic conditions, the study incorporates delay effects into simulations of the satellite's control system. The attitude control was initially modelled using the state-space approach. Three hybrid control strategies—PID-Lead, MPC-Lead, and MPC-PDLead—were then designed and evaluated for their effectiveness in managing the Roll (ϕ), Pitch (θ), and Yaw (ψ) axes. Performance was assessed using the Mean Square Error (MSE) as the primary metric under noisy conditions. Simulation results showed that all MPC-based controllers significantly outperformed the PID-Lead controller, achieving lower MSE values across all axes. Among them, the MPC-Lead and MPC-PDLead controllers demonstrated superior noise resilience and faster convergence to steady-state conditions. These findings suggest that MPC-based approaches offer a more robust and accurate solution for InnoSAT's attitude control, particularly under the influence of real-world disturbances.

Keywords: Attitude Control System, InnoSAT, Mean Square Error, MPC-Based Controllers

1.0 Introduction

In recent years, small satellites have become increasingly popular for research due to their affordability, compact size, simplified design, and energy efficiency. These characteristics make them a highly cost-effective solution for a wide range of applications. Technological advancements have further

enabled the development of small satellites for both practical use and academic study. Among these, the smallest categories, nanosatellites and picosatellites, are subsets of microsatellites, which are classified based on size and weight. To foster interest and expertise in satellite development among Malaysian universities, the National Space Agency (ANGKASA) introduced the Innovative Satellite (InnoSAT), a type of nanosatellite designed for educational and research purposes [1].

Attitude Control Systems (ACS) play a pivotal role in ensuring the stability, orientation, and overall success of satellite missions. These systems are responsible for maintaining or altering the satellite's orientation in space, enabling proper alignment of sensors, antennas, and solar panels concerning Earth or other celestial targets. Over the decades, the satellite attitude control problem has been extensively studied, resulting in a wide range of proposed solutions [1–15].

Classical control approaches, such as Proportional-Integral-Derivative (PID) controllers [2,3], remain popular due to their simplicity and ease of implementation. Mashor et al. [16] designed, developed, and implemented a PID control scheme for the InnoSAT attitude control system as part of a similar study. However, simulation results revealed that the PID controller exhibited inferior performance compared to the MPC-Lead and MPC-PDLead controllers [13], particularly in terms of longer settling time, higher overshoot, and reduced stability under time-delay conditions. These limitations highlight the challenges of using conventional PID control for high-precision satellite attitude control, especially when delays are present in the control loop. More sophisticated methods, including those based on Linear Matrix Inequality (LMI) formulations and Linear Quadratic Regulators (LQR) [4], offer improved performance by optimising control effort while maintaining system stability. Additionally, gain scheduling and linear parameter-varying techniques provide flexibility in adapting controller parameters based on the satellite's dynamic operating conditions. Model Predictive Control (MPC) [5–7] has emerged as a powerful alternative, particularly for handling multivariable systems with constraints. MPC's ability to predict future states of the system and optimise control inputs accordingly makes it highly suitable for complex satellite dynamics.

In parallel, artificial intelligence (AI)-based control strategies are gaining traction due to their ability to handle nonlinearities and uncertainties in satellite behaviour. Fuzzy logic controllers [8,9] offer robustness in the presence of imprecise or incomplete information, while neural networks [10,11] are capable of learning and adapting to changing system dynamics through data-driven approaches. These AI-driven techniques are particularly valuable in autonomous or deep-space missions where real-time human intervention is limited. Collectively, these developments reflect the continuous evolution of ACS technologies, driven by the increasing demands for precision, reliability, and autonomy in modern satellite missions. Following an in-depth investigation into the performance of Lead and Model Predictive Control (MPC) strategies, this study aims to develop a simulation framework to analyse the

behaviour and effectiveness of several hybrid attitude control configurations. These included PID-Lead, MPC-Lead, and MPC-PDLead controllers, allowing for a comparative assessment of their stability, responsiveness, and overall control performance in satellite applications.

2.0 Methodology

2.1 Equations of InnoSAT's Dynamic

The transfer function needs to be converted into state space. This transfer function is represented by Roll (ϕ), Pitch (θ), and Yaw (ψ), such as in (1), (2), and (3) [13][14].

$$\phi_{(s)} = \frac{s^2 + 0.3051s + 0.2040}{s^4 + 1.1050s^2 + 0.1650} \quad (1)$$

$$\theta_{(s)} = \frac{1}{s^2 - 7.1138 \times 10^{-3}} \quad (2)$$

$$\psi_{(s)} = \frac{s^2 - 0.3051s + 0.8088}{s^4 + 1.1050s^2 + 0.1650} \quad (3)$$

By (4) and (5) below, the general form of state-space is presented.

$$x_{k+1} = Ax_k + Bu_k + w_k \quad (4)$$

$$y_k = Cx_k + Du_k + v_k \quad (5)$$

A is the "state (or system) matrix," B is the "input matrix," C is the "output matrix," D is the "feedforward matrix," where x is the "state vector," y is the "output vector," u is the "input (or control) vector," and (in cases where the system model does not have a direct feedforward, D is the zero matrix). The equations (4) and (5) are also amended to include the state noise, w_k , and measurement noise, v_k .

2.2 Experimental setup

InnoSAT attitude controllers based on gap analysis are designed, developed, and compared in several steps. First, the state space technique is used to design and construct InnoSAT attitude controllers. Next, the performance of the suggested controllers for InnoSAT attitude control is compared. Additionally, this study comprised simulations under several operating parameters, including step input disturbance, measurement noise, one sample time delay, and varying gain. One kind of input is called a square input. The square wave input is displayed in Figure 1. Except for the periods from $t = 201$ sec to $t = 400$ sec and from $t = 601$ sec to $t = 800$ sec, when the input was set to +1, the square-wave input remained at -1.

Delay testing is a critical aspect of satellite controller validation due to the inherent communication latencies and processing delays present in space

missions. Given the physical distance between satellites and ground stations, signal transmission can introduce significant delays, necessitating autonomous decision-making by the onboard controller. Additionally, real-time control systems must remain stable and responsive despite delays in sensor feedback, actuator response, and inter-subsystem communication. Space-grade hardware, often constrained in computational power, may also contribute to processing lags, which can impact the performance of control algorithms such as PID or Kalman filters. Without proper delay testing, these delays could compromise system stability, lead to incorrect fault detection, or cause failures in coordinated subsystem operations. Therefore, rigorous delay testing is essential to ensure the controller's robustness, reliability, and safety under realistic operational conditions.

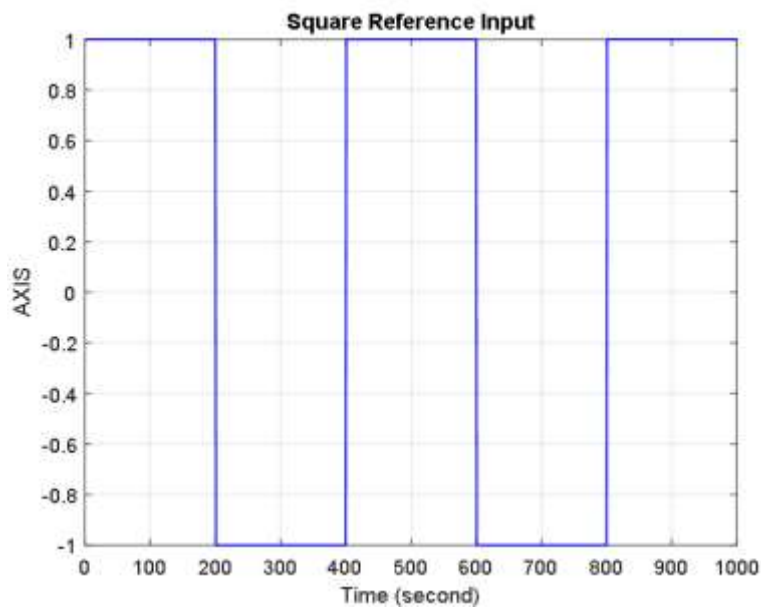


Figure 1: Square-wave input of normal condition from 0 sec to 1000 sec for the ACS InnoSAT plant

Time delay is a measure of how long a disturbance might last while a signal is being transmitted. In this document, paperwork $\tau = 1$, and the time delay is defined as paperwork τ the entire time delay. It will take some time for the system to react to the incoming reference signal. To comprehend the true dynamic behaviour of the satellite system and its entire performance, including stability, a time delay is crucial in satellite attitude control. Additionally, plants with time delays often have feedback controls that are overcompensated and unreliable. Equation (6) illustrates how the state space approach was applied in this study to measure the time delay utilising the input for the Roll (ϕ), Pitch (θ), and Yaw (ψ) axes.

$$x_{k+1} = Ax_k + Bu_{k-\tau} + 30.58T_{dx} + 5 \quad (6)$$

2.3 PID-Lead Controller Design

The term PID describes its three main components, a proportional control term (K_p), an integral control term (T_i), and a differential control term (T_{dd}) which was derived by Åström (2002), then $G_{cPID}(s)$ can be written as:

$$G_{cPID}(s) = K_p \left(1 + \frac{1}{T_i s} + \frac{T_{dd} s}{1 + (T_{dd}/N') s} \right) \quad (7)$$

The same thing happened as before to the PID-Lead controller, when $\frac{T_{dd} s}{1 + (T_{dd}/N') s}$ is set as T'_d , Equation (7) can be written as:

$$G_{cPID}(s) = K_p \left(1 + \frac{1}{T_i s} + T'_d \right) \quad (8)$$

The transfer function shown in Equation (8) is selected again and then multiplied by the Lead controller to achieve the PID-Lead controller, as shown in Figure 2.

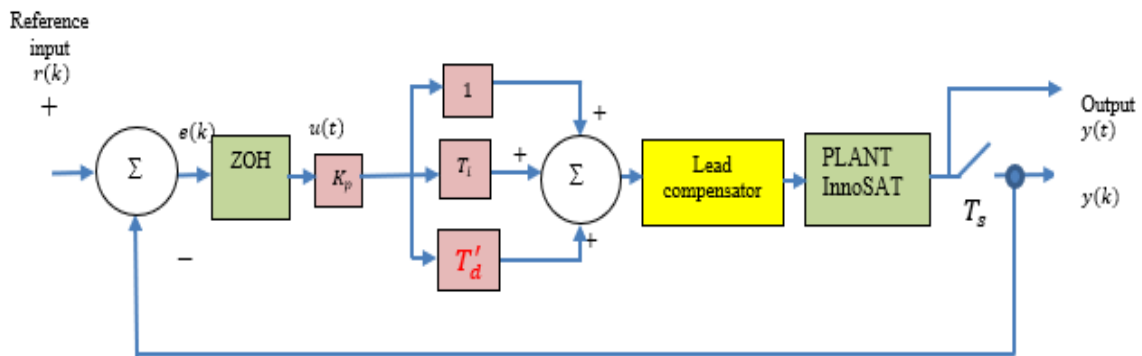


Figure 2: Block diagram of a PID-Lead controller for the InnoSAT plant

To create new transfer functions of the Roll (ϕ), Pitch (θ), and Yaw (ψ) axes, two controllers are coupled in series with the InnoSAT plant. The plant is then transformed into a discrete form. Only when the PID controller has been adjusted using the rule of thumb can the transfer equation be found [15]. Equation (7) represents the overall form of the PID-Lead controller in conjunction with the InnoSAT plant:

$$G_{PIDL}(s) = K_p \left(1 + T_i s + \left(\frac{T_{dd} s}{1 + (T_{dd}/N') s} \right) \right) \left(\frac{s+0.5}{s+5} \right) \quad (9)$$

The nonlinear InnoSAT plant is complicated to explain mathematically. However, it is known that sometimes it can be satisfactorily controlled by using a PID controller when the parameters are well-tuned. Three parameters that are used to establish the PID controller are K_p , T_i , and T_{dd} .

To find the values of the Roll (ϕ), Pitch (θ), and Yaw (ψ) axes for the PID-Lead

controller, K_p , T_i , and T_{dd} were tuned using the rule of thumb technique. K_p was initially set to the lowest amount and then gradually increased until it reached an unstable value during the steady-state condition. The outcome shows that at 0.1, the value of K_p achieved its highest state. T_i was then set to its lowest value and gradually increased until it reached its optimal value of 0.1. Finally, based on the output values of the rising time (t_r), settling time (t_s), and percentage overshoot. Then, T_{dd} was adjusted from zero to four since it demonstrated the best performance. For the Pitch (θ) and Yaw (ψ) axes, the steps were repeated. Table 1 contains all the observations.

Table 1: Tuned K_p , T_i and T_{dd} parameters for Roll (ϕ), Pitch (θ), and Yaw (ψ) axes of InnoSAT using PID-Lead controller

Parameter	Roll (ϕ) axis	Pitch (θ) axis	Yaw (ψ) axis
K_p	0.1	0.1	0.1
T_i	1	2	1
T_{dd} when $N=2$	4	8	4

2.4 MPC-Lead Controller Design

This study connected the controllers by connecting a lead controller in series with the MPC to enhance the control signal. The purpose of using a lead controller is to help MPC improve the systems. It also helps to stabilise the impact of MPC on sudden changes in the heading variable, $y(k)$. Additionally, the Lead Controller was used to mimic the insertion of a derivatives control term. It will increase the reaction's speed and bandwidth while reducing its overshoot. Figure 3 illustrates the series connection between the controller and MPC. The type of controller used in this investigation was the Lead Controller.

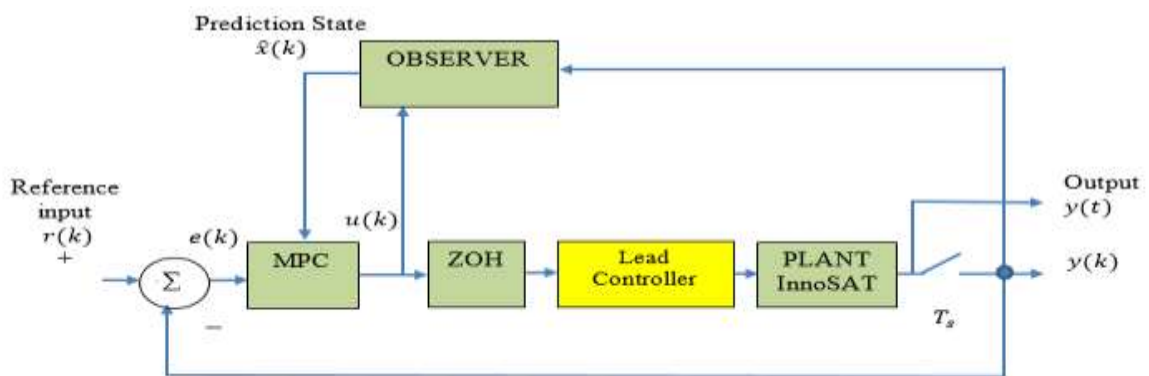


Figure 3: Block diagram of MPC-Lead Controller for the InnoSAT plant

The InnoSAT plant's performance was met by using the Lead Controller's chosen value for PID-Lead controllers. The new transfer functions of the Roll (ϕ), Pitch (θ), and Yaw (ψ) axes were then created by discretising equations (1), (2), and (3) of the InnoSAT plant using a 0.1-second sample period before being connected in series with the Lead Controller.

2.5 MPC-PDLead Controller Design

The MPC-based control methods were modified to achieve the necessary control performance in this investigation. The MPC-PDLead controller, which was based on the MPC-Lead controller, was created by adding the Lead Controller in series with the PD component. The same thing happened as before to the PD-Lead controller, when $\frac{T_{dd}s}{1+(T_{dd}/N)s}$ is set as T_{TOT} . Equation (7) can be written as:

$$G_{cPID}(s) = K_p(1 + T_{TOT}) \quad (10)$$

The design of the MPC-PDLead Controller is depicted in Figure 4.

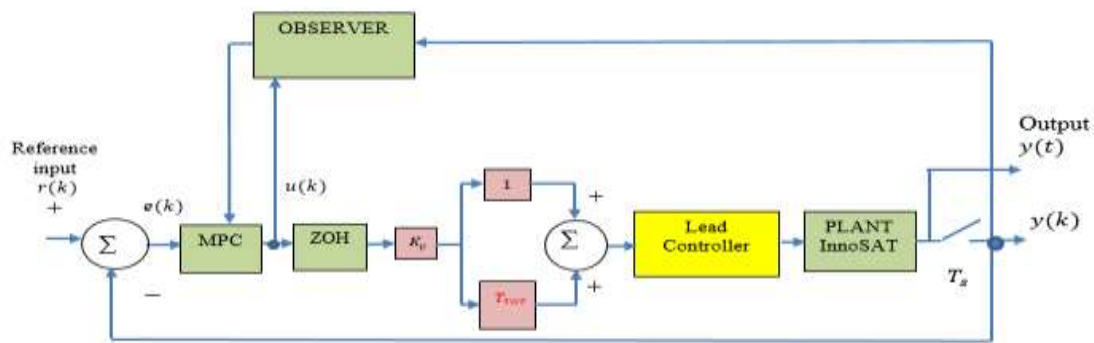


Figure 4: Block diagram of MPC-PDLead controller for the InnoSAT plant

A shorter rising time for the system to reach ideal conditions with the least amount of overshoot and the capacity to function as effectively as feasible to resume regular operations in the event of any anticipated disturbance are indicators of a strong controller's performance. The MPC-PDLead controller was cascaded with PD and Lead Controllers to get the necessary performance of the InnoSAT. This equation was converted to discrete form for the new transfer functions of Roll (ϕ), Pitch (θ), and Yaw (ψ) axes.

3.0 Results and Discussions

Figure 5 presents the Roll (ϕ) axis square response analysis, including both the full output and a zoomed-in view, for three different controllers—PID-Lead, MPC-Lead, and MPC-PDLead—under the influence of a time delay. The figure illustrates both the system response and the corresponding error for each controller configuration. Among the three, the MPC-Lead controller initially exhibited the fastest response. However, it also experienced the highest maximum overshoot, reaching 73.65% around the 80-second mark. Despite this, it successfully converged to zero by approximately 88 seconds. The MPC-PDLead controller showed a more moderate behaviour, with a peak overshoot of 46.83% occurring near 90 seconds. It settled more quickly than MPC-Lead, stabilising around 28.8 seconds. In contrast, the PID-Lead controller demonstrated the slowest performance, with the longest rise time recorded at 16 seconds and a peak overshoot of 35.86%. It required

significantly more time—approximately 156.3 seconds—to fully converge to zero. These results suggest that while MPC-based controllers respond more rapidly, they may introduce higher overshoot without careful tuning. The MPC-PDLead offers a balance between speed and stability, whereas the PID-Lead controller, though exhibiting less initial overshoot, suffers from a considerably slower settling time.

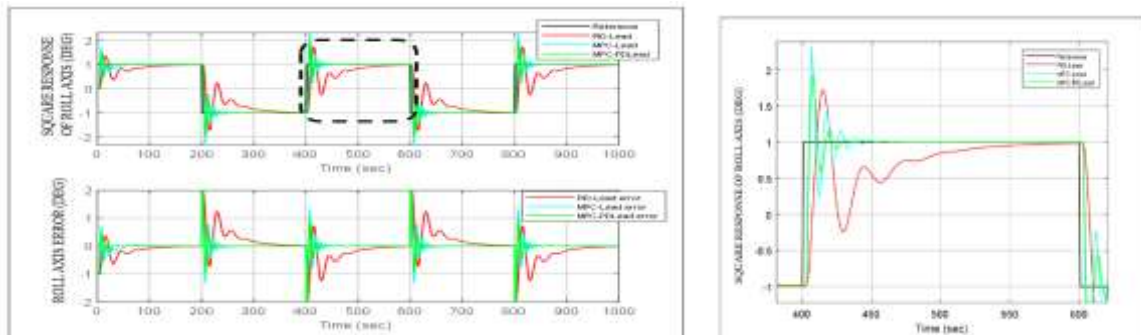


Figure 5: Performance Comparison square response and the zoom-out of Roll (ϕ) axis using a variety of controllers (with delay=1)

Figure 5 indicates the zoomed-out output of the Roll (ϕ) axis square response using three types of controllers (PID-Lead, MPC-Lead, and MPC-PDLead) with a delay effect. Three controllers saw an increase in the maximum overshoot value, according to the observation made during this second positive cycle. The controller with the largest maximum overshoot, 131.95% after 7s, was the MPC-Lead, despite having the smallest time rise. In the 5.02 seconds, the MPC-Lead had converged to zero. The second-highest rise time value was recorded by the MPC-PDLead, which had a maximum overshoot of 93.76% after 6 seconds. At 33.1 seconds, this controller similarly achieved a steady-state condition. After 15, the PID-Lead controller had the second-highest maximum overshoot value (72.72%) and the biggest time rise, which has the slowest settling time (183.2s).

Figure 6 presents the output and zoomed-out output of Pitch (θ) Axis square response analysis using three types of controllers (PID-Lead, MPC-Lead, and MPC-PDLead) with a delay effect. Figure 7 shows the outputs and errors for the outputs of each type of controller used. Figure 6 also shows that at an initial time, the highest overshoot for PID-Lead was 49.58% after 24 seconds, 67.73% for MPC-Lead after 8 seconds, and 42.1% for MPC-PDLead after 8 seconds. In the meantime, MPC-PDLead needed 24 seconds to reach the settling time criteria, followed by MPC-Lead controller (50.1 seconds) and PID-Lead (58 seconds).

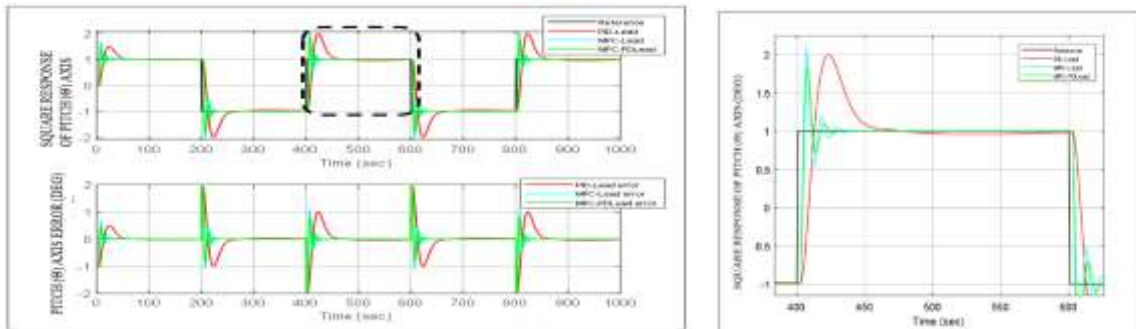


Figure 6: Performance comparison of square response and the zoom-out of Pitch (θ) axis using a variety of controllers (with delay=1)

Figure 6 depicts the zoom-out output of the Pitch (θ) axis square response analysis using three types of controllers (PID-Lead, MPC-Lead, and MPC-PDLead) with a delay effect. According to the observation, the maximum overshoot value for each of these controller types increased during the positive second cycle of the squared response. Despite having a very high maximum overrun of 100% after 23 seconds, the PID-Lead was, as usual, the fastest-rising time controller. MPC-Lead had the second-highest speed, with a maximum overshoot of 110.49% after 7 seconds. It takes 28.8 seconds for MPC-PDLead, 35.3 seconds for MPC-Lead controller, and 193.1 seconds for PID-Lead to reach the settling time condition.

Figure 7 reveals the output and zoomed-out output of Yaw (ψ) Axis square response analysis using three types of controllers (PID-Lead, MPC-Lead, and MPC-PDLead) with delay. The outputs and errors for each type of controller employed are displayed in Figure 7. The MPC-Lead had the smallest time rise at the beginning of the positive first cycle, but after 8 seconds, it overshoot to a maximum of 77.71%. The second-fastest, MPC-PDLead, comes next, with a better maximum overshoot of 44.83% following the 9s. The controller with the biggest time rise, the PID-Lead, had a significant maximum overrun of 56.5% after 18 seconds. The settling time was 97.4 seconds for PID-Lead, 105.5 seconds for MPC-Lead, and 28.2 seconds for MPC-PDLead.

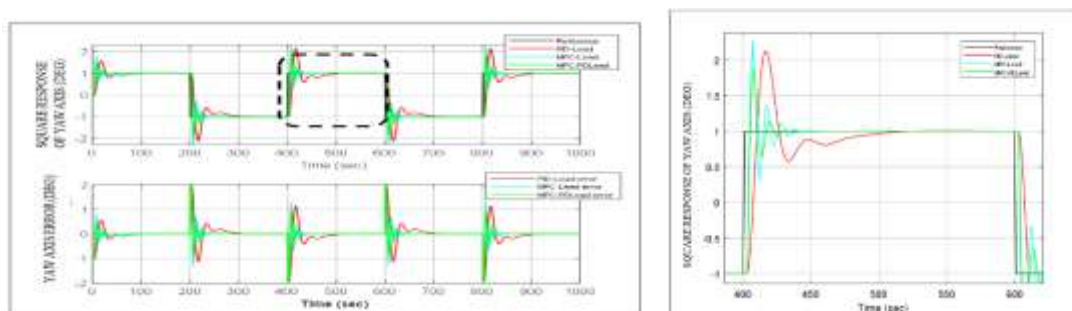


Figure 7: Performance comparison square response and the zoom-out of the Yaw (ψ) axis using a variety of controllers (with delay=1)

Figure 7 observes the zoom-out output of the Yaw (ψ) Axis square response analysis using three types of controllers (PID-Lead, MPC-Lead, and MPC-PDLead) with a delay effect. According to the observation, the MPC-PDLead controller had the lowest maximum overshoot of 89.6% after 8 seconds, as indicated by the initial response condition of the positive second cycle. After 16 seconds, the PID-Lead's maximum overshoot rose to 113%. Finally, after 16 seconds, the PID-Lead has a maximum overrun of 113%. MPC-PDLead took the quickest (28.1s) to reach the steady-state condition, followed by MPC-Lead (44.3s) and PID-Lead (104.9s).

In satellite attitude control, the Mean Square Error (MSE) is commonly employed as a primary cost function to evaluate control system accuracy. Its sensitivity to large deviations makes it particularly useful for highlighting performance differences and enabling quantitative comparisons between various control strategies. For instance, [17] proposed a fault-tolerant attitude tracking controller designed to handle uncertainties, environmental disturbances, and actuator faults. The controller's effectiveness was assessed using angular error metrics, achieving a settling time of 7 seconds and maintaining an error margin below 4%. Similarly, another study [18] applied a Nonlinear Model Predictive Control (NMPC) approach combined with a deep learning framework to suppress satellite antenna vibrations. This approach demonstrated a marked improvement in control accuracy and system stability, as evidenced by a significant reduction in Root Mean Square Error (RMSE). Additionally, research on the optimal synthesis of satellite control systems [19] highlighted the importance of minimising the mean square error as a key criterion for designing energy-efficient and high-performance controllers. Collectively, these studies underscore the critical role of MSE and RMSE not only as objective performance metrics but also as essential tools in tuning and optimising control algorithms to enhance the accuracy, robustness, and reliability of satellite systems.

Figures 5 through 8 present the output responses of Roll (ϕ), Pitch (θ), and Yaw (ψ) axes as well as the mean squared error values, which are tabulated in Table 2. Nonetheless, the percentage of overshoot marginally rises when MPC-Lead and PID-Lead controllers experience overrun rates greater than 20%. For example, the MPC controller's beginning condition differs from the 20% maximum overshoot. Lastly, the MPC controller with PD and Lead components had been successful in significantly reducing the mean square error for each of the three axes, as shown by the Roll (ϕ), Pitch (θ), and Yaw (ψ) axes output responses of MSE with delay time in Table 2.

Table 2: MSE for a variety of controllers (with delay=1) from $t = 0$ s to $t = 1000$ s

Controllers	Mean Square Error (MSE)		
	Roll (ϕ) axis	Pitch (θ) axis	Yaw (ψ) axis
PID-Lead	2.1322×10^{-01}	1.7688×10^{-01}	1.5083×10^{-01}
MPC-Lead	8.0310×10^{-02}	6.9454×10^{-02}	7.6173×10^{-02}
MPC-PDLead	7.1080×10^{-02}	6.9641×10^{-02}	6.9286×10^{-02}

4.0 Conclusion

This study presented three advanced control strategies—PID-Lead, MPC-Lead, and MPC-PDLead—for satellite attitude control, grounded in the satellite's dynamic model. Among the proposed methods, the MPC-Lead controller exhibited superior performance, achieving optimal balance between responsiveness, noise attenuation, and overall system stability. While all controllers demonstrated a consistent time delay, the MPC-based variants—particularly MPC-Lead—were significantly more effective at counteracting noise disturbances than the PID-Lead controller. These findings underscore the enhanced adaptability and robustness of model predictive control approaches in dynamic satellite environments. For future enhancement, the integration of the InnoSAT design system into a real-time Graphical User Interface (GUI) is proposed. A GUI would enable dynamic command sequencing, real-time response visualisation, and a more intuitive interaction with the control system. Such a development would streamline simulation workflows, enhance validation accuracy under mission-like conditions, and support more agile prototyping and operational testing.

Acknowledgement

The authors would like to express their sincere gratitude to the Ministry of Higher Education Malaysia for the opportunity and financial support provided for the completion of this research. Special thanks are also extended to the Pusat Penyelidikan dan Inovasi, Jabatan Pendidikan Politeknik dan Kolej Komuniti, and Politeknik Tuanku Sultanah Bahiyah for their valuable technical support, guidance, and assistance throughout this study.

Author Contributions

Fadzilah Hashim: Conceptualisation, Methodology, Data Curation, Formal Analysis, Writing – Original Draft, Writing – Review & Editing;

Siti Maryam Sharun: Co-Supervision, Writing – Review & Editing;

Mohd Yusoff Mashor: Conceptualisation, Validation, Supervision, Resource, Writing – Reviewing and Editing;

Nor Hasrimin Md Nor: Writing – Reviewing and Editing.

Conflicts of Interest

The manuscript has not been published elsewhere and is not under consideration by any other journal. All authors have approved the review, agree with its submission and declare that there are no conflicts of interest in the manuscript.

References

- [1] F. Hashim, M. Y. Mashor, Z. Osman, and N. H. Zainol, "Comparison of lead-controller and PID-lead controller to control InnoSAT attitude system," *Politeknik & Kolej Komuniti Journal of Engineering and Technology*, vol. 8, no. 1, pp. 25–36, 2023.
- [2] A. Bello, K. S. Olfe, J. Rodríguez, J. M. Ezquerro, and V. Lapuerta,

- "Experimental verification and comparison of fuzzy and PID controllers for attitude control of nanosatellites," *Advances in Space Research*, vol. 71, no. 9, pp. 3613–3630, 2023.
- [3] Y. Shan, L. Xia, and S. Li, "Design and simulation of satellite attitude control algorithm based on PID," in *Journal of Physics: Conference Series*, vol. 2355, no. 1, p. 012035, Oct. 2022, IOP Publishing.
- [4] E. U. Enejor, F. M. Dahunsi, K. F. Akingbade, and I. O. Nelson, "Low Earth orbit satellite attitude stabilization using linear quadratic regulator," *European Journal of Electrical Engineering and Computer Science*, vol. 7, no. 3, pp. 17–29, 2023.
- [5] S. Aslam, Y. C. Chak, M. H. Jaffery, R. Varatharajoo, and Y. Razoumny, "Deep learning-based fuzzy-MPC controller for satellite combined energy and attitude control system," *Advances in Space Research*, vol. 74, no. 7, pp. 3234–3255, 2024.
- [6] R. J. Caverly, S. Di Cairano, and A. Weiss, "Electric satellite station keeping, attitude control, and momentum management by MPC," *IEEE Transactions on Control Systems Technology*, vol. 29, no. 4, pp. 1475–1489, 2020.
- [7] R. Rodrigues, A. Murilo, R. V. Lopes, and L. C. G. De Souza, "Hardware-in-the-loop simulation for model predictive control applied to satellite attitude control," *IEEE Access*, vol. 7, pp. 157401–157416, 2019.
- [8] M. Navabi and S. Hosseini, "A hybrid PSO fuzzy-MRAC controller based on EULERINT for satellite attitude control," in *Proc. 2020 8th Iranian Joint Congress on Fuzzy and Intelligent Systems (CFIS)*, Sep. 2020, pp. 033–038.
- [9] M. Navabi, N. S. Hashkavaei, and M. Reyhanoglu, "Satellite attitude control using optimal adaptive and fuzzy controllers," *Acta Astronautica*, vol. 204, pp. 434–442, 2023.
- [10] M. Raja, K. Singh, A. Singh, and A. Gupta, "Design of satellite attitude control systems using adaptive neural networks," *INCAS Bulletin*, vol. 12, no. 3, pp. 173–182, 2020.
- [11] A. R. Fazlyab, F. F. Saberi, and M. Kabganian, "Adaptive attitude controller for a satellite based on neural network in the presence of unknown external disturbances and actuator faults," *Advances in Space Research*, vol. 57, no. 1, pp. 367–377, 2016.
- [12] G. Garg and V. Garg, "Design and application of lead compensator to a guided missile system," in *Proc. International Conference on Emerging Trends in Engineering and Technology (ICETET)*, 2013.
- [13] F. Hashim, *Design of InnoSAT Attitude Controller Based on Model Predictive Control Approach*, Master's Thesis, Universiti Malaysia Perlis, Faculty of Electrical Engineering and Technology, 2024.
- [14] F. Hashim, M. Y. Mashor, and S. M. Sharun, "Full- and reduced-order compensator for InnoSAT attitude control," *Jurnal Teknologi*, vol. 76, no. 12, 2015.
- [15] S. Skogestad, "Probably the best simple PID tuning rules in the world," in *Proc. AIChE Annual Meeting*, Reno, NV, USA, Nov. 4–9, 2001.

- [16] M. Y. Mashor and M. C. Mahdi, "Performance of manual and auto-tuning PID controller for unstable plant–nano satellite attitude control system," in *Proc. 6th International Conference on Cyber and IT Service Management (CITSM)*, Aug. 2018, pp. 1–5.
- [17] A. Hatami, S. A. Pourmohammad, and A. Ghasemi, "Disturbance-tolerant attitude tracking controller for uncertain satellites under actuator faults and saturation," *Aerospace Science and Technology*, vol. 147, p. 108403, 2025.
- [18] Y. Eltanahy and S. K. Elangovan, "Vibration control of satellite antenna using NMPC and deep learning-based system identification," *ISA Transactions*, vol. 142, pp. 752–764, 2024.
- [19] V. A. Babaev and I. G. Lisichkin, "Optimization synthesis of satellite control system with a solar sensor," *Russian Aeronautics*, vol. 67, no. 5, pp. 635–642, 2024.